

# Interrelation between antiferromagnetic and superconducting gaps in high- $T_c$ materials

E. Arrigoni, M. G. Zacher, T. Eckl, and W. Hanke

*Institut für Theoretische Physik, Universität Würzburg, Am Hubland, 97074 Würzburg, Germany*

We propose a phenomenological model, comprising a microscopic SO(5) model plus the on-site Hubbard interaction  $U$  (“projected SO(5) model”) to understand the interrelation between the  $d$ -wave-gap modulation observed by recent angle-resolved photoemission experiments in the insulating antiferromagnet  $\text{Ca}_2\text{CuO}_2\text{Cl}_2$  and the  $d$ -wave gap of high- $T_c$  superconducting materials. The on-site interaction  $U$  is important in order to produce a Mott gap of the correct order of magnitude, which would be absent in an exact SO(5) theory. The projected SO(5) -model explains the gap characteristics, namely both the symmetry and the different order of magnitude of the gap modulations between the antiferromagnetic and the superconducting phases. Furthermore, it is shown that the projected SO(5) theory can provide an explanation for a recent observation [E. Pavarini et al., Phys. Rev. Lett. 87, 47003 (2001)], i. e. that the maximum  $T_c$  observed in a large variety of high- $T_c$  cuprates scales with the next-nearest-neighbor hopping matrix element  $t'$ .

71.30.+h, 71.10.Fd, 71.10.Hf

## I. INTRODUCTION

The SO(5) theory has been proposed as a unified description of antiferromagnetism (AF) and  $d$ -wave superconductivity (SC) in the high- $T_c$  materials<sup>1</sup>. While originally formulated as a phenomenological effective field theory for the global phase diagram of the high- $T_c$  cuprates, it was soon realized that the SO(5) symmetry, in contrast to the more common spin SU(2) symmetry, is not realized exactly in strongly-correlated models, such as the  $t - J$  and Hubbard model. However, it can be detected, under some circumstances, in the *low-energy sector* of such models<sup>2-7</sup>. This seems to indicate that this symmetry, which is broken at the microscopic level, may be restored, at least approximately, at long distances and low energies.

Recently, it was pointed out that an exact formulation of the SO(5) theory cannot properly account for the large Mott-insulating gap which is present at half filling in the high- $T_c$  cuprates: an SO(5) transformation “rotates” spin into charge and, thus, an exactly SO(5) -invariant system should have the same charge and spin gap, in contrast to the actual situation for the high- $T_c$  materials. This prompted for an improved formulation of the original idea by introducing a Gutzwiller “projection” onto states where the constraint of no double occupancy is implemented locally<sup>8,9</sup>. In particular, a so-called “projected” SO(5) *bosonic* model has been explicitly constructed<sup>8</sup>. It is built up out of five bosons, three triplets which “condense” at low temperature into the antiferromagnetic state and two charged bosons, i. e. Cooper pairs, which condense into the superconducting state. The “high-energy” doubly occupied charged boson states are then projected out from the Hilbert space. The central hypothesis of the projected-SO(5) (p-SO(5)) theory is that the model is accurate in describing both the static

and dynamic properties in the high- $T_c$  superconductors (HTSC).

On the basis of a numerically exact Quantum-Monte-Carlo (QMC) calculation of the p-SO(5) bosonic model, it has recently indeed been shown that this model gives a realistic description of the phase diagram of the HTSC materials and properly accounts for many of their physical properties<sup>10</sup>. Among those are the neutron-scattering resonance, which appears as a Goldstone mode in the p-SO(5) description, as well as an unusual chemical potential dependence on doping found in the prototype material  $\text{La}_{2-x}\text{Sr}_x\text{CuO}_4$ <sup>11</sup>, which signals a possible (microscopic) phase separation<sup>12</sup>. One crucial point of this bosonic p-SO(5) model is that, on the basis of a newly implemented Stochastic Series Expansion QMC technique, it can be simulated up to unprecedented system sizes of about  $10^4$  sites, which is more than one order of magnitude larger than corresponding fermionic QMC simulations. This fact allowed, for the first time, for an approximate “finite-size-study” of the p-SO(5) bosonic model in the three-dimensional case, and for extracting the “scaling properties” close to the bicritical (AF-SC) point. The numerical results point to a partial asymptotic restoring of the SO(5) symmetry at this critical point, i. e. at long distances. This is very interesting, since the projection destroys the symmetry at the Hamiltonian level (The Hamiltonian no longer commutes with the SO(5) generators). While the mean-field classical p-SO(5) Hamiltonian of Ref. 8 conserves its SO(5) invariant form, quantum fluctuations break the symmetry. However, as shown in Ref.<sup>13</sup>, at finite temperature quantum fluctuations become less and less important, and one can hope that symmetry-breaking effects due to the projection become asymptotically irrelevant in the neighborhood of a finite-temperature critical point, which is what the numerical results seem to find.

Therefore, one part of our motivation to study the p-

SO(5) model on the *fermionic level* stems from the success of the bosonic model. Thus, in the present paper, we start again from the assumption that the high- $T_c$  materials are characterized by an underlying approximate SO(5) symmetry. This assumption is further supplemented by the Gutzwiller “projection”, i. e. the Hubbard- $U$ -term provides an important additional ingredient to the SO(5)-symmetric part of the Hamiltonian, which guarantees the presence of a Mott gap at half-filling. In this sense, we choose our Hamiltonian as the simplest (namely scalar SO(5) invariant<sup>14</sup>) Hamiltonian, which possesses such a symmetry and which displays the correct  $d$ -wave superconducting gap at finite doping. The physical basis is thus the assumption of a *projected* SO(5) symmetry, and the existence of a superconducting state at finite doping. The  $t - J$  model was shown by our previous numerical studies<sup>3</sup> to have (nearly) projected SO(5) symmetry in the bosonic sector. However, the  $t - J$  model cannot explain the  $|d|$ -wave AF gap modulation in the fermionic sector, it therefore misses an important piece of physics our current model contains (unless one introduces *ad-hoc* values for longer-ranged hoppings  $t', t''$ , see below). Thus, the logic of our approach is to construct an effective model, which matches the low-energy experiments, rather than trying to derive an effective model from first principle. This is the central idea behind a Landau-type approach to strongly-correlated systems, and can be very useful, although not complete.

This brings us to the second part of our motivation. It is the relation to recent angle-resolved photoemission data, which found evidence for a  $d$ -wave-like modulation of the antiferromagnetic gap, suggesting an intimate interrelation between the AF insulator and the SC with its  $d$ -wave gap. In a recent letter<sup>9</sup> it was shown, that the projected SO(5) theory correctly describes the observed gap characteristics. Specifically, it accounts for the order of magnitude difference between the AF gap modulation of order  $J \approx 0.2$  eV) and the SC gap ( $\sim J/10$ ) and is also consistent with the  $d$ -wave gap dispersion. Thus the projection is crucial, since in an exactly SO(5)-invariant model, the  $d$ -wave SC gap would be transformed into a pure  $|d|$ -wave AF gap with the same amplitude and without a constant ( $s$ -wave) part. In Ref. 9, the on-site Hubbard  $U$  has been treated by a Hartree-Fock decoupling, unifying the gap interrelation in the much-used spin-density-wave (SDW) picture for the AF and BCS limit for the SC. This treatment will be relegated here to a short appendix (Sec. A), introducing some notations and also giving a simple illustration of the crucial difference the “projection”, i. e. the  $U$ -term induces in the AF gap modulation and in its SC counterpart. In the present paper, we concentrate on a more controlled calculation for larger  $U$  ( $U \gg t$ ), i.e. a slave-boson calculation.

This paper is organized as follows:

In Sec. II, we start with a summary of the experimental results observed by angular-resolved photoemission spectroscopy (ARPES), which have motivated our cal-

culational. In Sec. III, we show that the  $\pi$ -operators of the SO(5) symmetry “rotate” the  $d$ -wave symmetry of the SC order parameter into the  $|d|$ -wave symmetry of the AF order parameter. This argument is general, and independent of the details (in particular, it survives the projection). More specifically then, we discuss the possibility of introducing a generalized form factor  $g_k$  for the SO(5) symmetry, which emphasizes the importance of longer-ranged pairings in accordance with the experimental observations. The comparison of our results with ARPES experiments is given in Sec. III C. In Sec. IV we compare the mean-field result with a slave-boson approach. The treatment of the antiferromagnetic and of the superconducting phase are given in Sec. IV A and IV B, respectively. The usually employed  $t'-(t'')$  fitting procedure in Hubbard- $(t - J)$ -like models to ARPES data seems, at first sight, to be completely uncorrelated with the experimental finding, which emphasizes the universal role of the magnetic energy scale  $J$ , namely the fact that the insulating bandwidth itself is of order  $J$ . In Sec. III B, we show that the  $t' - t''$ -hoppings can indeed arise effectively from the SO(5) part of the Hamiltonian, i. e. from the spin interaction term. Since in the SO(5) description these hoppings scale with the SC strength ( $V$  in Eq. 10), they are also qualitatively in line, from a rather different point of view, with a recent observation<sup>15</sup> i.e. that the maximum  $T_c$  observed in a variety of HTSC scale with the next-nearest-neighbor hopping matrix element  $t'$ . This empirical observation and its p-SO(5) interpretation will be discussed in Sec. III B. Finally, Sec. V gives a summary of our results.

## II. EXPERIMENTAL GUIDELINES

Our analysis is motivated by recent ARPES experiments by the Stanford group<sup>16</sup>, which indicate an intimate interrelation between the superconducting and antiferromagnetic state. These experiments show remnants of a superconducting gap in the half-filled high- $T_c$  parent compound  $\text{Ca}_2\text{CuO}_2\text{Cl}_2$ . The ARPES gap structure in the AF phase is given by the dots with error bars in Fig. 1 of Ref. 9. It displays a  $d$ -wave-like, i.e.  $|\cos k_x - \cos k_y|$ -like dispersion in the one-electron spectral function  $A(\mathbf{k}, \omega)$  with respect to the lowest energy state at wave-vector  $\mathbf{k} = (\pi/2, \pi/2)$ . The points show a  $d$ -wave dispersion function of the photoemission band along the edge of the magnetic Brillouin zone, which, by assuming a symmetric inverse photoemission band, can be understood as a modulation of the single-particle Mott-Hubbard gap. The inset of this figure presents the ARPES data and the dispersion features in a two-dimensional plot: on a line drawn from the center of the Brillouin zone to the experimental points, the distance between these points to the intersection of this line with the AF Brillouin zone gives the value of the dispersion at the  $\mathbf{k}$ -point considered. The data closely follow the

$|\cos k_x - \cos k_y|$ -behavior, depicted in the  $d$ -wave full line. The important point is that these photoemission data suggest that the  $d$ -wave-like dispersion in the insulator is also the underlying reason for the pseudogap in the underdoped regime: this "high-energy" pseudogap of the order  $J \sim 0.1\text{eV}$  continuously evolves out of the insulating feature, as documented not only by the same energy scale but again by the same  $d$ -wave dispersion<sup>17</sup>. Since, on the other hand, this high-energy feature is closely correlated to the superconducting gap as a function of both doping and momentum<sup>18,17,19</sup>, we conclude that a microscopic theory should be able to explain the interrelation between the superconducting gap and the AF gap modulation. In Ref. 9, we have shown that a SO(5) model plus  $U$  provides such an interrelation in a natural way. In the present paper, we want to discuss this issue in more detail.

### III. MICROSCOPIC MODEL

As discussed above, an important point missing in an exact SO(5) theory is the correct description of the Mott-gap at half-filling. For this reason, it is important to account for the strong on-site Coulomb repulsion  $U$ . This can naturally be done by including the usual Hubbard on-site interaction term  $U$  "by hand". Formally, one can project out doubly-occupied sites by taking  $U \rightarrow \infty$ , eventually. This should be a good approximation since these states are separated by an energy scale, which is orders of magnitude higher than the interesting low-energy scales set by the Néel ( $T_N$ ) and by the superconducting ( $T_c$ ) transition temperatures. The idea of such a "projected" SO(5) theory, recently formulated in a rigorous

fashion for *bosonic* degrees of freedom in Ref. 8, is visualized in Fig. 1.

As already mentioned in the Introduction, the physical basis for the choice of our Hamiltonian is the *assumption* that the high- $T_c$  materials are following an underlying SO(5) symmetry. The hamiltonian in Eqs. (13-17) has been chosen as the simplest SO(5)-symmetric hamiltonian that can properly reproduce the  $d$ -wave superconducting state of the High- $T_c$  materials in a BCS mean-field description. Our starting point is the superconducting state. We then perform an SO(5) rotation on the operator level that introduces the magnetic part of the interaction [second term in Eq. 13]. The resulting hamiltonian is then SO(5) invariant. This hamiltonian must be further supplemented with the projection (Hubbard- $U$ ) term and the usual chemical potential term.

Our aim is to describe the peculiar ARPES results of Ref. 16 by the simple assumption of SO(5) symmetry of the microscopic Hamiltonian *plus* the projection prescription. The first task is, thus, to build up the *simplest* fermionic lattice Hamiltonian obeying these two requirements. The part of the Hamiltonian leading to the superconducting state is dictated by experiments on the SC gap in the cuprates. These experiments suggest a  $d$ -wave superconducting gap resulting in a nearest neighbor  $d$ -wave BCS interaction. We also allow for more general forms of the SC gap function, including longer-range interactions, as observed in more accurate ARPES experiments on  $\text{Bi}_2\text{Sr}_2\text{CaCu}_2\text{O}_{8+\delta}$ <sup>20</sup>. With the SC part of the Hamiltonian being fixed, the AF part is then also fixed by the SO(5) rotation. Therefore, once the form of the wavefunction in the SC state is given, *the SO(5) assumption allows to make a prediction about the AF state.*

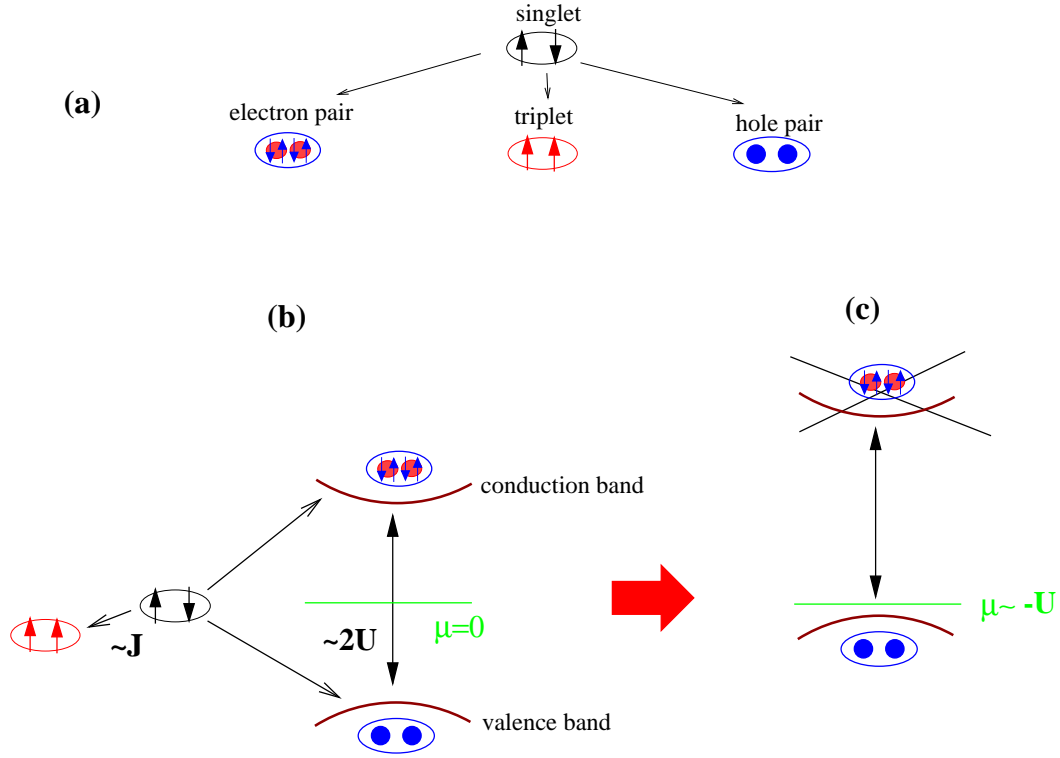


FIG. 1. Suppose one starts from some singlet state<sup>1,21</sup> as a description of the vacuum [e.g. a resonating-valence-bond-like (RVB) state], and looks for excitations on top of it. In an (ideal) exact SO(5) –symmetric description (a), triplet–, hole–pair– and electron–pair–excitations on top of this RVB state are equivalent. This condition is obviously violated in the cuprate materials at half filling where spin–excitations are gapless (due to the antiferromagnetic state), while hole–/electron–pair excitations have a large gap of the order of the Mott gap (b). A projected SO(5) theory, however, can restore the equivalence between spin and charge excitations *in the hole sector*. This is done by lowering the chemical potential to the top of the valence band, and projecting out high-energy electron-pair excitations so that hole-pair excitations become gapless (c).

To see this, let us consider the operator creating a Cooper pair with vanishing total momentum:

$$P(\mathbf{k}) \equiv \frac{i}{2} c_{\mathbf{k}} \sigma^y c_{-\mathbf{k}}, \quad (1)$$

where  $c_{\mathbf{k}} = (c_{\mathbf{k},\uparrow}, c_{\mathbf{k},\downarrow})$  is a two-component destruction operator for an electron with momentum  $\mathbf{k}$ , and  $\sigma^\alpha$  are the usual Pauli matrices ( $\alpha = x, y, z$ ). An SO(5) rotation is generated by the  $\pi$  operator<sup>1,14,22</sup>

$$\pi_\alpha = \sum_{\mathbf{k}} g_{\mathbf{k}} c_{\mathbf{k}+\mathbf{Q}} \sigma^\alpha \sigma^y c_{-\mathbf{k}}, \quad (2)$$

with the form factor

$$g_{\mathbf{k}} = \text{sgn}(\cos k_x - \cos k_y). \quad (3)$$

The  $\pi$  operator rotates the Cooper pair into the magnon operator

$$N_\alpha(\mathbf{k}) \equiv \frac{1}{2} c_{\mathbf{k}+\mathbf{Q}}^\dagger \sigma^\alpha c_{\mathbf{k}}, \quad (4)$$

via the commutation rules

and

$$[\pi_\alpha, N_\beta(\mathbf{k})] = -i \delta_{\alpha,\beta} g_{\mathbf{k}} P(\mathbf{k}), \quad (5)$$

$$[\pi_\alpha^\dagger, P(\mathbf{k})] = i g_{\mathbf{k}} N_\alpha(\mathbf{k}). \quad (6)$$

From Eq. (5) and Eq. (6) it is clear that a  $d$ -wave Cooper pair  $d_{\mathbf{k}}P(\mathbf{k})$  with the nearest-neighbor gap dispersion

$$d_{\mathbf{k}} = (\cos k_x - \cos k_y). \quad (7)$$

transforms into a “ $|d|$ -wave-shape” magnon  $|d_{\mathbf{k}}|N_\beta(\mathbf{k})$ , giving a corresponding “ $|d|$ -wave” gap in the AF state. In its original formulation, an SO(5) rotation was defined by the  $\pi$  operator, Eq. (2), with the “nearest-neighbor” form factor Eq. (3). From the above discussion it is clear that such a formulation is only appropriate for a similarly nearest-neighbor superconducting gap function, Eq. (7). An extended gap, as found in recent ARPES experiments on  $\text{Bi}_2\text{Sr}_2\text{CaCu}_2\text{O}_{8+\delta}$ <sup>20</sup> would not be transformed

into the appropriate AF form by this SO(5) transformation. However, Eq. (3) is not the only possible form of the form factor which can be used. In fact, one can use a *different* SO(5) symmetry transformation with a *more general* form of  $g_{\mathbf{k}}$ . More specifically, it can be shown that the  $\pi$  operator Eq. (2) satisfies the closure requirement of the SO(5) group as long as the form factor has the properties  $|g_{\mathbf{k}}| = 1$ , and  $g_{\mathbf{k}+\mathbf{Q}} = -g_{-\mathbf{k}}$ . Thus, given a more general form of the gap dispersion  $d_{\mathbf{k}}$  satisfying  $d_{\mathbf{k}+\mathbf{Q}} = -d_{-\mathbf{k}}$ , one can choose

$$g_{\mathbf{k}} = \text{sgn } d_{\mathbf{k}}. \quad (8)$$

A gap function satisfying these requirements can support, e. g., third-neighbor terms:

$$d_{\mathbf{k}} = b(\cos k_x - \cos k_y) + (1 - b)(\cos 3k_x - \cos 3k_y). \quad (9)$$

From the commutators, Eq. (5) and Eq. (6), it is thus clear that the generalized choice Eq. (8) produces a corresponding AF gap function of the form  $|d_{\mathbf{k}}|$ .

As explained above, our procedure starts by taking the simplest fermionic lattice Hamiltonian reproducing the appropriate  $d$ -wave state in the SC state within a BCS (mean-field) description. This is given by

$$H_{SC} = H_{kin} + \frac{V}{2N} [\Delta \Delta^\dagger + \Delta^\dagger \Delta], \quad (10)$$

where the kinetic-energy term reads

$$H_{kin} = \sum_{p,\sigma} \varepsilon_p c_{p,\sigma}^\dagger c_{p,\sigma}. \quad (11)$$

Here,  $\varepsilon_p$  is the single-particle kinetic energy, and  $\Delta$  the  $d$ -wave pairing operator

$$\Delta \equiv \sum_{\mathbf{k}} d_{\mathbf{k}} P(\mathbf{k}). \quad (12)$$

with  $P(\mathbf{k})$  given by Eq. (1).

The second term on the right-hand side of Eq. (10) describes a coupling between Cooper pairs. The SO(5) assumption requires that, (i), a corresponding coupling between magnons be present as well, which leads to the form

$$H_{SO(5)} = H_{SC} - \frac{V}{N} \mathbf{m} \cdot \mathbf{m}, \quad (13)$$

where

$$m_\alpha \equiv \sum_{\mathbf{k}} |d_{\mathbf{k}}| N_\alpha(\mathbf{k}), \quad (14)$$

and, (ii), that  $\varepsilon_{p+Q} = -\varepsilon_{-p}$ , which suggests the simple nearest-neighbor form  $\varepsilon_p = -2t(\cos p_x + \cos p_y)$ .

As discussed in the Introduction, restricting to a purely SO(5)-symmetric Hamiltonian like Eq. (13), would produce a gap with nodes in the AF state and no constant

part of the Mott-insulating gap, as present in the high- $T_c$  materials. For this reason, our Hamiltonian must be supplemented with a term suppressing double occupation at half filling. This can be achieved by introducing the usual on-site Hubbard-repulsion term

$$H_U = U \sum_{\mathbf{r}} \left( n_{\mathbf{r},\uparrow} n_{\mathbf{r},\downarrow} - \frac{1}{2} \sum_{\sigma} n_{\mathbf{r},\sigma} \right), \quad (15)$$

where,  $n_{\mathbf{r},\sigma} \equiv c_{\mathbf{r},\sigma}^\dagger c_{\mathbf{r},\sigma}$  is the particle number with spin  $\sigma$  on site  $\mathbf{r}$ . and for convenience, we have subtracted a constant chemical-potential term. Clearly, for a *complete* suppression one should take the  $U \rightarrow \infty$  limit. However, here we will consider a finite  $U = 8t$  giving a more physical *partial* projection resulting in a finite Mott gap at half filling. It is clear that, concerning the energy scales of the order  $J$  we are interested in, there is very little difference between results at  $U/t = 8$ , and  $U/t = \infty$ . This will be confirmed by our calculation later, see Fig. 2.

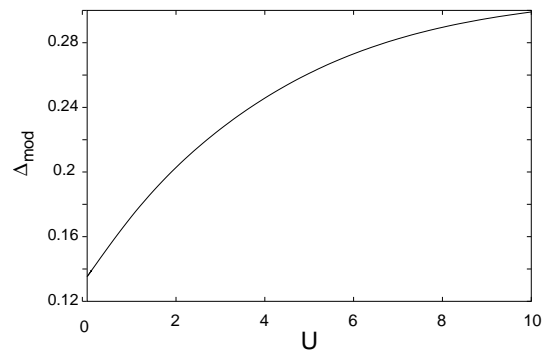


FIG. 2. The amplitude  $\Delta_{\text{mod}}$  of the AF  $d$ -wave-like modulation as a function of the Hubbard-interaction  $U$  for fixed  $V = 0.61t$  and  $b = 1$ . The figure plots the results of the slave-boson calculation of Sec. IV.

The last term in the Hamiltonian is the usual chemical potential term  $H_\mu$  controlling the doping, i. e.

$$H_\mu = -\mu \sum_{\mathbf{r},\sigma} c_{\mathbf{r},\sigma}^\dagger c_{\mathbf{r},\sigma}. \quad (16)$$

In total, our Hamiltonian has the form

$$H_{tot} = H_{SO(5)} + H_U + H_\mu. \quad (17)$$

In Ref. 13, we have shown that the chemical potential term partially compensates for the SO(5) symmetry breaking of the Hubbard term  $H_U$  (see also schematic Fig. 1c), as also shown for the  $t - J$  model in Ref. 3.

The interacting part of  $H_{SO(5)}$  is a special case of the manifestly SO(5) invariant part introduced by Rabello et al.<sup>14</sup>:

$$H_{\text{SO}(5),I} \equiv H_{\text{SO}(5)} - H_{\text{kin}} = \sum_{a=1}^5 \sum_{\mathbf{k}, \mathbf{k}', \mathbf{q}} V_1(\mathbf{k}, \mathbf{k}', \mathbf{q}) \times \left( \Psi_{\mathbf{k}}^\dagger \Gamma^a \Psi_{\mathbf{k}+\mathbf{q}} \right) \left( \Psi_{\mathbf{k}'}^\dagger \Gamma^a \Psi_{\mathbf{k}'-\mathbf{q}} \right), \quad (18)$$

where

$$\Psi_{\mathbf{k}} = \left\{ c_{\mathbf{k},\uparrow}, c_{\mathbf{k},\downarrow}, g(\mathbf{k})c_{-\mathbf{k}+\mathbf{Q},\uparrow}^\dagger, g(\mathbf{k})c_{-\mathbf{k}+\mathbf{Q},\downarrow}^\dagger \right\}, \quad (19)$$

is an SO(5) spinor, and the  $\Gamma$  matrices

$$\Gamma^1 = \begin{pmatrix} 0 & -i\sigma^y \\ i\sigma^y & 0 \end{pmatrix}, \quad \Gamma^{2,3,4} = \begin{pmatrix} \sigma^{x/y/z} & 0 \\ 0 & \sigma^{x/y/zT} \end{pmatrix} \\ \Gamma^5 = \begin{pmatrix} 0 & \sigma^y \\ \sigma^y & 0 \end{pmatrix}, \quad (20)$$

provide the SO(5) group structure. In particular, our exactly SO(5) invariant part of the Hamiltonian, Eq. (13) is given by Eq. (18) with the simple choice

$$V_1(\mathbf{k}, \mathbf{k}', \mathbf{q}) = -\frac{V}{16N} |d_{\mathbf{k}}| |d_{\mathbf{k}'}| \delta_{\mathbf{q}, \mathbf{Q}}, \quad (21)$$

Our “minimal” projected SO(5) model contains, in principle, five parameters, although only two of them are adjustable. The adjustable parameters are the interaction term  $V$ , and  $b$  [cf. Eq. (9)].  $V$ , due to the SO(5) condition, controls the magnitude of both the interactions between Cooper pairs and between magnons. As anticipated, we fix this parameter by fitting the experimental magnitude of the gap in the SC phase. The second one,  $b$ , is needed when the SC gap deviates from the nearest-neighbor form. This parameter can be fitted by the detailed form of the gap in the SC phase. The other three parameters,  $\mu$ ,  $t$ , and  $U/t$ , are not free.  $\mu$  is fixed by the hole density, which we take from the experiments to be  $\langle n \rangle = 0.89^{20}$  in the SC phase, while for  $t$  we take the commonly accepted value  $t = 0.5\text{eV}$ . Several experiments and theoretical fittings agree about a strong-coupling value of  $U$  of the order  $U/t \approx 8$ . On the other hand, we show that our results saturate in the large- $U$  limit, i. e. they are practically independent of  $U$  for  $U/t \gtrsim 8$ .

We now proceed to illustrate the mean-field treatment of our Hamiltonian Eq. (17). The main point of this treatment is to (a) show that the  $|d|$ -modulation survives the Gutzwiller projection. This important property further clarifies what is meant by “projected SO(5) symmetry” in the fermionic sector, generalizing the concept introduced in Ref.<sup>8</sup>. Furthermore, we show (b) that the SO(5) projection introduces a difference in the magnitude of the superconducting and antiferromagnetic gap modulation which is consistent with the experiment. This quantitative analysis is more model dependent compared to point (a), but within the approximations we show the robustness of the result.

Details of the SDW treatment of the antiferromagnetic phase and of the BCS treatment of the superconducting phase as well as some basic notations can be found in the appendix, Sec. A.

## A. Discussion of the SDW solution

Eq. (A5) yields the coupled set of self-consistent equations:

$$\Delta_{\text{mod}} = \frac{V}{2N} \sum_{\mathbf{k}} |d_{\mathbf{k}}| \frac{\Delta_{\text{mod}} |d_{\mathbf{k}}| + \Delta_U}{E(\mathbf{k})}, \quad (22)$$

$$\Delta_U = \frac{U}{2N} \sum_{\mathbf{k}} \frac{\Delta_{\text{mod}} |d_{\mathbf{k}}| + \Delta_U}{E(\mathbf{k})}, \quad (23)$$

where  $E(\mathbf{k})$  is the quasiparticle energy given in Eq. A11, and where the sum runs again over the *whole* Brillouin zone. The behavior of  $\Delta_U$  and of ratio  $\Delta_{\text{mod}}/\Delta_{\text{SC}}$  are reported in Fig. 3. As one can see, the ratio between the AF and SC gaps, which is unity at the exactly SO(5) - symmetric point  $U/t = 0$ , increases with  $U$  and saturates at  $U/t \approx 8$ .

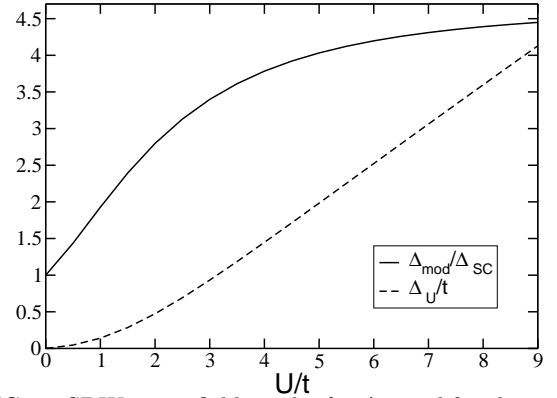


FIG. 3. SDW mean-field results for  $\Delta_U$  and for the ratio of the  $d$ -wave-like modulated parts of the gap  $\Delta_{\text{mod}}/\Delta_{\text{SC}}$  (both at half filling) as a function of  $U$ .

We now study the gap structure of the single-particle spectrum along the magnetic zone boundary. Since the free dispersion vanishes here, the gap becomes

$$\Delta_{\text{AF}}(\mathbf{k}) = E^v(\mathbf{k}) - E^c(\mathbf{k}) = 2(\Delta_U + |d_{\mathbf{k}}| \Delta_{\text{mod}}). \quad (24)$$

We, thus, obtain a  $d$ -wave-like modulation with amplitude  $2\Delta_{\text{mod}}$  on top of the constant Hubbard gap  $2\Delta_U$ , as anticipated above. This gap structure is represented schematically in Fig. (4).

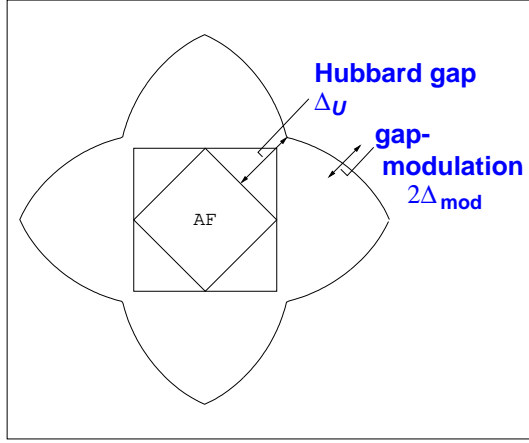


FIG. 4. Schematic gap structure in the AF phase along the magnetic zone boundary. On a line drawn from the center of the Brillouin zone to any point on the curve, the distance from this point to the intersection of the line with the antiferromagnetic Brillouin zone boundary gives the gap at the  $\mathbf{k}$ -point of the intersection. On top of the constant Hubbard gap, which, for convenience, has been reduced in scale, there is a  $d$ -wave like modulation.

### B. Physical interpretation of the SO(5) -generated (long-range) magnetic interaction part

It is instructive to transform the magnon term Eq. (14) entering the magnetic part of the interaction (last term on the r.h.s. of Eq. (13)) into real space. This gives

$$\mathbf{m} = \sum_{\mathbf{r}} \mathbf{m}(\mathbf{r}), \quad (25)$$

where the Néel order parameter at site  $\mathbf{r}$  reads

$$m_{\alpha}(\mathbf{r}) = \frac{1}{2} \sum_{\mathbf{r}_2} w(\mathbf{r} - \mathbf{r}_2) e^{i\mathbf{Q}\mathbf{r}_2} c_{\mathbf{r}}^{\dagger} \sigma^{\alpha} c_{\mathbf{r}_2}, \quad (26)$$

and has an extended internal structure given by the Fourier transform  $w(\mathbf{r})$  of  $|d_{\mathbf{k}}|$ . This function is given by (cf. Ref. 14)

$$w(m\mathbf{a}_x + n\mathbf{a}_y) = \frac{4}{\pi^2} \frac{1 + (-1)^{m+n}}{[(m+n)^2 - 1][(m-n)^2 - 1]}. \quad (27)$$

We want to show how, at the mean-field level, the extended structure of the magnetic part of the SO(5) - symmetric Hamiltonian leads to effective longer-ranged hopping terms similar to the commonly used values. These terms can be explicitly seen in the mean-field SO(5) -symmetric Hamiltonian in real space

$$[H_{\text{SO}(5)}]_{MF} = -\Delta_{\text{mod}} \sum_{\mathbf{r}, \mathbf{r}', \sigma} \sigma w(\mathbf{r} - \mathbf{r}') e^{i\mathbf{Q}\mathbf{r}} c_{\mathbf{r}, \sigma}^{\dagger} c_{\mathbf{r}', \sigma} + H_{SC}. \quad (28)$$

Notice that the effective hopping terms only connect sites within the same sublattice, since  $w(\mathbf{r} - \mathbf{r}')$  vanishes otherwise. Furthermore, the sign of the effective hopping matrix elements is opposite for spin up and down, as well as for the two sublattices, thus yielding an identical sign for the majority spin species on each sublattice i.e. for the electrons whose spin is polarized along the direction of the staggered magnetic field. The processes involving those "majority" electrons are the most important ones since the ratio between the number of "major" to "minor" electrons is

$$N_{\text{major}}/N_{\text{minor}} = (1 + \langle m \rangle)/(1 - \langle m \rangle), \quad (29)$$

where  $\langle m \rangle = \frac{\Delta U}{U}$  is the mean-field staggered magnetization which is of the order  $\langle m \rangle \approx \frac{1}{2}$ .

The effective second- and third-nearest neighbor "hopping amplitudes" generated by the interaction Eq. (28) are

$$t' = \Delta_{\text{mod}} \frac{-8}{3\pi^2} \approx -0.08t, \quad (30)$$

$$t'' = \Delta_{\text{mod}} \frac{8}{9\pi^2} \approx +0.03t, \quad (31)$$

$$t''/t' = -1/3. \quad (32)$$

Here we have used the self-consistent solution  $\Delta_{\text{mod}} \approx 0.3t$  for large  $U$  and the results of Sec. A 2. These effective second- and third-nearest neighbor hopping elements have the same sign but are somewhat smaller than the ones commonly introduced in order to correctly reproduce the Fermi-surface topology of typical high- $T_c$  materials (see, e. g., Ref. 23). Nevertheless, here, these "effective" parameters are obtained without any fitting to the experiments by the simple assumption that leads us to the projected SO(5) Hamiltonian Eq. (17). This makes clear, in particular, that the gap modulation is related to the magnetic energy scale  $J$ , as demonstrated in the ARPES experiments and repeatedly stressed in the literature<sup>24</sup>. Eq. (28) also contains longer-ranged hopping processes which, however, are much smaller than  $t'$  and  $t''$ . These long-range terms, however, produce the cusp-like feature of the antiferromagnetic gap modulation which has been observed in ARPES experiments on  $\text{Ca}_2\text{CuO}_2\text{Cl}_2$ <sup>16</sup>.

Since the hoppings Eq. (30) scale with the strength of the SO(5) coupling ( $V$  in Eq. 10), and since, at least in the weak-coupling regime  $V \ll 8t$  the superconducting  $T_c$  increases with  $V$ , one can expect that  $T_c$  is an increasing function of the next-nearest-neighbor hopping  $t'$ . This fact has been observed in a recent analysis of Pavarini *et al.*<sup>15</sup>, who have plotted the maximum  $T_c$  as a function of the ratio  $t'/t$  for different compounds. As explained above, our theory provides a *qualitative* explanation for such a behavior. This is more quantitatively

shown in Fig. 5, which plots our  $T_c$  versus  $t'$  results in the upper part. Here, different next-nearest-neighbor hoppings  $t'$  have been extracted by varying the SO(5) coupling  $V$ . For a given  $V$ , and thus  $t'$ ,  $T_c$  has then been extracted from the weak-coupling BCS equation, which is valid for  $V \lesssim 8t$ . The lower part of Fig. 5 gives finally the  $T_c$  versus  $t'$  results of Pavarini *et al.*<sup>15</sup> for a large variety of HTSC materials.

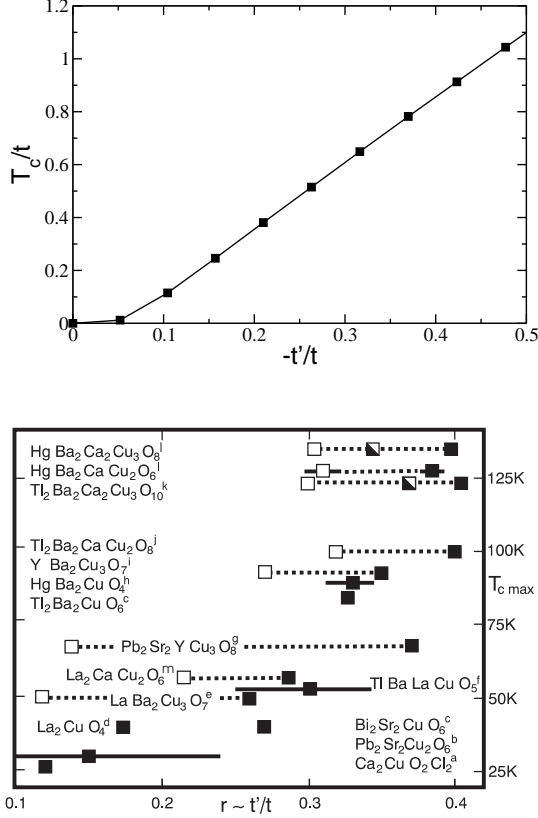


FIG. 5. Correlation between  $T_c$  and the next-nearest-neighbor hopping  $t'$  (in units of  $t$ ). The top figure reports the results of our calculation for, whereby different  $t'$  are obtained by varying  $V$ , and the superconducting  $T_c$  is evaluated via the weak-coupling BCS equation. The doping is fixed at 15% ( $\langle n \rangle = 0.85$ ),  $U = 8t$ , and  $b = 1$ . For comparison, the bottom figure shows the results of Ref. 15 for different materials.

### C. Discussion of ARPES experiments

The interesting point is that the structure of the AF gap Eq. (24), shown in Fig. 4 is a consequence of the SO(5) -symmetry principle combined with the effect of the Hubbard interaction  $U$ . This gap structure has recently been measured in the undoped (half-filled) cuprate parent compound  $\text{Ca}_2\text{CuO}_2\text{Cl}_2$ <sup>16</sup>. Fig. 1 of Ref. 9 shows the ARPES results for the AF gap modulation on this material, in comparison with our result, Eq. (24). The

experimental figure displays the peak dispersion versus the  $d$ -wave-like function  $|\cos k_x - \cos k_y|$ . The very good fit to a straight line shows that the dispersion is  $d$ -wave-like with a characteristic "cusp" at momentum  $\mathbf{k} = (\pi/2, \pi/2)$ .

Concerning the energy scales that are observed in the experiment<sup>16</sup>, the authors find a modulation  $\Delta_{\text{mod}}$  of the order the magnetic exchange coupling  $J$  which is about one order of magnitude higher than the experimentally observed amplitude of the superconducting gap  $\Delta_{\text{SC}} \approx J/10$ . This is a second, most important point that would be difficult to understand in terms of an "exact" SO(5) symmetry, which would be expected to preserve the amplitude of the modulation by "rotating" from the SC to the AF gap. However, the result of our *projected* SO(5) calculation is that the difference by one order of magnitude between the two amplitudes is correctly reproduced, and it is due to the projection as well. This can be seen from Fig. (3), displaying the ratio  $\Delta_{\text{mod}}/\Delta_{\text{SC}}$  as obtained by our mean-field calculation as a function of the Hubbard repulsion  $U$ . We see that for large  $U \approx 8t$  the AF gap modulation  $\Delta_{\text{mod}}$  is approximately four times larger than the superconducting gap  $\Delta_{\text{SC}}$ , when the latter is also calculated at half filling. An additional factor two emerges from the doping dependence of  $\Delta_{\text{SC}}$  shown in Fig. (6) so that the total ratio of  $\Delta_{\text{mod}}/\Delta_{\text{SC}}$  becomes of the order of 8.

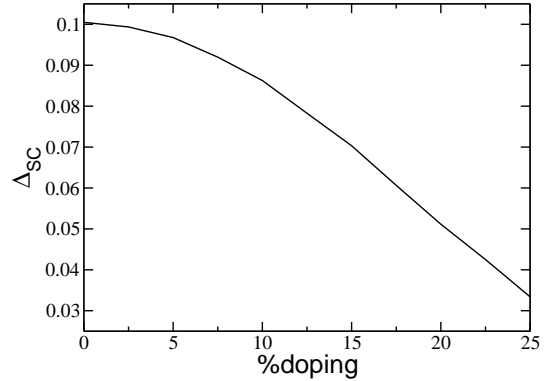


FIG. 6. Mean-field result for the  $d$ -wave SC gap  $\Delta_{\text{SC}}$  obtained by solving the gap equation (A1) as a function of doping  $(1 - \langle n \rangle)$  for  $V = 0.8t$  and  $b = 1$ . At a doping of  $\approx 20\%$ ,  $\Delta_{\text{SC}}$  takes the value  $\Delta_{\text{SC}} \approx 0.05t$  which is about the correct order of magnitude for the high- $T_c$  materials ( $\Delta_{\text{SC}} \approx J/10$ ).

At first sight, it might seem difficult to understand why the introduction of  $U$  changes the order of magnitude of the SC and AF gap modulations, despite the fact that both are controlled by the same energy scale  $V$ . This can be easily understood at weak coupling  $V \ll t$  and for  $U \gg t$ . In this case, the usual BCS gap equation Eq. (A1) – which does not depend on  $U$  – gives  $\Delta_{\text{SC}} \sim \exp[-\text{const.}/(n_F V)]$ , i. e. it decreases *exponentially* with small  $V$ . On the other hand, the AF gap equation, Eq. (22), *does* depend on  $U$ . In fact, for large



$U$ ,  $E(\mathbf{k}) \approx \Delta_U \propto U$ , which inserted in Eq. (22) gives  $\Delta_{mod} \propto V$ , i. e.  $\Delta_{mod}$  behaves *linearly* with  $V$ , totally different from  $\Delta_{SC}$ .

Our “projected” SO(5) symmetry principle, thus, can provide an explanation of the interrelation between the SC and the AF gap both qualitatively, via the same dispersion, as well as semiquantitatively, i. e. via the correct order of magnitude difference between the two modulations.

#### IV. SLAVE-BOSON APPROACH

The Hartree-Fock treatment described in the previous section was physically motivated as a natural first step to show the connection of the SDW with the BCS solutions via a SO(5) theory. Our motivation for introducing the Hubbard repulsion  $U$  was to project out states containing doubly occupied sites and therefore to account for the Mott gap at half filling. However, within the Hartree-Fock treatment discussed above, the Hubbard interaction is treated only perturbatively, which might be questionable for large values of  $U$ . For this reason, we repeat the calculation using an extension of the Kotliar-Ruckenstein slave-boson approach<sup>25–28</sup> which, while still requiring a mean-field approximation, is more appropriate to deal with the strong repulsion  $U$ .

Confidence in this approximation derives from various observations: (i) This method is known to give rather satisfying agreement with QMC results over a wide range of Coulomb correlations  $U$  and values for the doping<sup>29</sup>. (ii) The two main results of our study, namely, that the AF gap modulation is correlated to the SC gap by symmetry and that the Hubbard term  $H_U$  induces the order of magnitude difference in these effects should be independent of specific approximations, at least *qualitatively*. This will be explicitly verified by comparing with the simple Hartree-Fock study described above.

Within the Slave-boson formalism for the Hubbard model one introduces four bosons  $e_{\mathbf{r}}^{(\dagger)}$ ,  $p_{\mathbf{r},\sigma}^{(\dagger)}$ , and  $d_{\mathbf{r}}^{(\dagger)}$ , for each lattice site  $\mathbf{r}$ , corresponding to empty, singly occupied site with spin  $\sigma$ , and to doubly-occupied sites, respectively. Creation and annihilation of a fermion  $c_{\mathbf{r},\sigma}$  is mapped onto the creation and annihilation of a pseudo fermion  $f_{\mathbf{r},\sigma}$  with an appropriate boson, according to the mapping:

$$\begin{aligned} c_{\mathbf{r},\sigma}^{\dagger} &\longrightarrow f_{\mathbf{r},\sigma}^{\dagger} z_{\mathbf{r},\sigma}^{\dagger} \\ c_{\mathbf{r},\sigma} &\longrightarrow z_{\mathbf{r},\sigma} f_{\mathbf{r},\sigma} \end{aligned} \quad (33)$$

Kotliar and Ruckenstein have shown that, while a certain degree of arbitrariness is allowed in the choice of the bosonic operator  $z_{\mathbf{r}}$ , the choice

$$\begin{aligned} z_{\mathbf{r},\sigma} &= (1 - d_{\mathbf{r}}^{\dagger} d_{\mathbf{r}} - p_{\mathbf{r},\sigma}^{\dagger} p_{\mathbf{r},\sigma})^{-\frac{1}{2}} (e_{\mathbf{r}}^{\dagger} p_{\mathbf{r},\sigma} + p_{\mathbf{r},-\sigma}^{\dagger} d_{\mathbf{r}}) \\ &\quad (1 - e_{\mathbf{r}}^{\dagger} e_{\mathbf{r}} - p_{\mathbf{r},-\sigma}^{\dagger} p_{\mathbf{r},-\sigma})^{-\frac{1}{2}}, \end{aligned} \quad (34)$$

turns out to give the correct free fermion limit for  $U \rightarrow 0$  at the mean-field level. In addition, it was shown<sup>28</sup> that Eq. (34) gives the correct non-interacting limit at all orders in the fluctuation ( $1/N$ ) expansion as well. Restriction to the *physical* Hilbert space is achieved by projecting out unphysical states. In a functional-integral formalism this is taken care of by integrating over *Lagrange* multipliers  $\lambda_{\mathbf{r}}^{(1)}, \lambda_{\mathbf{r},\sigma}^{(2)}$  for each site  $\mathbf{r}$ <sup>25</sup>. The total effective Hamiltonian is thus given by Eq. (17), whereby the Fermi fields have undergone the transformation Eq. (33), plus the Lagrange multiplier terms:

$$\begin{aligned} H_{eff} &= H_{tot} + \sum_{\mathbf{r}} i \lambda_{\mathbf{r}}^{(1)} \left( e_{\mathbf{r}}^{\dagger} e_{\mathbf{r}} + \sum_{\sigma} p_{\mathbf{r},\sigma}^{\dagger} p_{\mathbf{r},\sigma} + d_{\mathbf{r}}^{\dagger} d_{\mathbf{r}} - 1 \right) \\ &+ \sum_{\mathbf{r},\sigma} i \lambda_{\mathbf{r},\sigma}^{(2)} (f_{\mathbf{r},\sigma}^{\dagger} f_{\mathbf{r},\sigma} - p_{\mathbf{r},\sigma}^{\dagger} p_{\mathbf{r},\sigma} - d_{\mathbf{r}}^{\dagger} d_{\mathbf{r}}) \end{aligned} \quad (35)$$

##### A. Antiferromagnetic phase

At the lowest order, the functional integral can be treated by means of a saddle-point approximation, whereby the bosonic fields are replaced by time-independent complex numbers. In the antiferromagnetic phase, one has the usual two-sublattices saddle point solution, i.e.

$$\begin{aligned} d_{\mathbf{r}}(\tau) &= d, \\ e_{\mathbf{r}}(\tau) &= e, \\ p_{\mathbf{r},\sigma}(\tau) &= p_1 + e^{i\mathbf{Q}\mathbf{r}} \sigma p_2, \\ \lambda_{\mathbf{r}}^{(1)} &= i\lambda_1, \\ \lambda_{\mathbf{r},\sigma}^{(2)} &= i\lambda_2 + ie^{i\mathbf{Q}\mathbf{r}} \sigma \lambda_3, \end{aligned} \quad (36)$$

from which it follows that

$$z_{\mathbf{r},\sigma}(\tau) = z_1 + e^{i\mathbf{Q}\mathbf{r}} \sigma z_2, \quad (37)$$

where  $d, e, p_1, p_2, \lambda_1, \lambda_2, \lambda_3, z_1, z_2$  can be chosen to be real numbers.

The effective slave-boson mean-field Hamiltonian becomes

$$\begin{aligned} H_{SBMF} &= N\lambda_1 e^2 - N\lambda_1 + 2N(p_1^2 + p_2^2)(\lambda_1 - \lambda_2) \\ &- 4N\lambda_3 p_1 p_2 + \lambda_1 N d^2 + N U d^2 - 2N\lambda_2 d^2 \\ &+ \sum_{\mathbf{k},\sigma} f_{\mathbf{k},\sigma}^{\dagger} (\lambda_2 - \mu) f_{\mathbf{k},\sigma} + \lambda_3 \sum_{\mathbf{k},\sigma} \sigma f_{\mathbf{k}+\mathbf{Q},\sigma}^{\dagger} f_{\mathbf{k},\sigma} \\ &+ (z_1^2 + z_2^2) \sum_{\mathbf{k},\sigma} \varepsilon(\mathbf{k}) f_{\mathbf{k},\sigma}^{\dagger} f_{\mathbf{k},\sigma} + H_{\text{SO}(5),I}. \end{aligned} \quad (38)$$

The slave-boson approach can only be applied to deal with the on-site repulsion part  $U$ , while the SO(5) part of the interaction  $[H_{\text{SO}(5),I}]$ , cf. Eq. (18) will still be treated by the Hartree-Fock decoupling, as in Eq. (A4). This is appropriate, since the SO(5) interaction

is assumed to be relatively weak (of the order of  $J$ ) in contrast to the large Hubbard repulsion  $U$ . In our procedure, we *first* carry out the Hartree-Fock decoupling of the SO(5) interaction part of the Hamiltonian, and *then* apply the slave-boson mapping Eq. (33). In this way, in the AF phase, we have

$$H_{\text{SO}(5),I} = \sum_{\mathbf{k},\sigma} \Delta_{\mathbf{k}}^{(4)} \sigma c_{\mathbf{k},\sigma}^\dagger c_{\mathbf{k}+\mathbf{Q},\sigma}, \quad (39)$$

with

$$\Delta_{\mathbf{k}}^{(4)} = -\frac{V}{2N} |d_{\mathbf{k}}| \sum_{\mathbf{k}',\sigma} |d_{\mathbf{k}'}| \sigma \langle c_{\mathbf{k}',\sigma}^\dagger c_{\mathbf{k}+\mathbf{Q},\sigma} \rangle. \quad (40)$$

The transformation, Eq. (33), with the saddle-point values Eq. (36) can then be applied to Eq. (39) by first transforming into real space. Going back to momentum space yields

$$H_{\text{SO}(5),I} = \sum_{\mathbf{k},\sigma} \Delta_{\mathbf{k}}^{(4)} \sigma \left\{ (z_1^2 + z_2^2) f_{\mathbf{k},\sigma}^\dagger f_{\mathbf{k}+\mathbf{Q},\sigma} + 2z_1 z_2 \sigma f_{\mathbf{k},\sigma}^\dagger f_{\mathbf{k},\sigma} \right\} \quad (41)$$

We can now insert the SO(5) interaction in Eq. (41) into the Slave-boson Hamiltonian Eq. (38), and obtain

$$\begin{aligned} H_{\text{SBMF}} &= \sum_{\mathbf{k},\sigma} f_{\mathbf{k},\sigma}^\dagger f_{\mathbf{k},\sigma} \\ &\times \left[ \varepsilon(\mathbf{k})(z_1^2 - z_2^2) - \mu + \lambda_2 + 2\Delta_{\mathbf{k}}^{(4)} z_1 z_2 \right] \\ &+ \sum_{\mathbf{k},\sigma} f_{\mathbf{k},\sigma}^\dagger f_{\mathbf{k}+\mathbf{Q},\sigma} \left[ \lambda_3 \sigma + \Delta_{\mathbf{k}}^{(4)} \sigma (z_2^2 + z_1^2) \right] + H_{bos} \\ &= \sum_{\mathbf{k},\sigma}^{\text{AF}} \begin{pmatrix} f_{\mathbf{k},\sigma} \\ f_{\mathbf{k}+\mathbf{Q},\sigma} \end{pmatrix}^\dagger \begin{pmatrix} \eta_1(\mathbf{k}) & \eta_2(\mathbf{k}) \\ \eta_2(\mathbf{k}) & \eta_3(\mathbf{k}) \end{pmatrix} \begin{pmatrix} f_{\mathbf{k},\sigma} \\ f_{\mathbf{k}+\mathbf{Q},\sigma} \end{pmatrix} \\ &+ H_{bos}, \end{aligned} \quad (42)$$

with

$$\begin{aligned} \eta_1(\mathbf{k}) &= \varepsilon(\mathbf{k})(z_1^2 - z_2^2) - \mu + \lambda_2 + 2\Delta_{\mathbf{k}}^{(4)} z_1 z_2 \\ \eta_2(\mathbf{k}) &= \lambda_3 \sigma + \Delta_{\mathbf{k}}^{(4)} \sigma (z_2^2 + z_1^2) \\ \eta_3(\mathbf{k}) &= -\varepsilon(\mathbf{k})(z_1^2 - z_2^2) - \mu + \lambda_2 + 2\Delta_{\mathbf{k}}^{(4)} z_1 z_2, \end{aligned} \quad (43)$$

where  $H_{bos}$  is a purely bosonic part. Diagonalization of Eq. (42) yields the eigenvalues

$$\begin{aligned} E_{\pm}(k) &= \lambda_2 - \mu + 2\Delta_{\mathbf{k}}^{(4)} z_1 z_2 \pm \left\{ \lambda_3^2 + \varepsilon(\mathbf{k})^2 (z_1^2 - z_2^2)^2 \right. \\ &\quad \left. + 2\Delta_{\mathbf{k}}^{(4)} \lambda_3 (z_1^2 + z_2^2) + (\Delta_{\mathbf{k}}^{(4)})^2 (z_1^2 + z_2^2)^2 \right\}^{\frac{1}{2}} \end{aligned} \quad (44)$$

Although Eq. (44) seems to break the particle-hole symmetry at half filling, this is not the case. Indeed the self-consistent solution yields at half filling  $\lambda_2 - \mu =$

$z_2 = 0$ , which makes the expression particle-hole symmetric. Eq. (44) describes the gap structure: Since along the magnetic zone boundary the tight-binding dispersion  $\varepsilon(\mathbf{k})$  is identical to zero, the dispersion along the magnetic zone boundary reads at half filling:

$$E_{2/1}(\mathbf{k}) = \pm \lambda_3 + \Delta_{\mathbf{k}}^{(4)} z_1^2. \quad (45)$$

Therefore, we obtain a constant part of the gap  $\Delta_U = 2\lambda_3$  plus a modulation

$$\Delta_{\mathbf{k}}^{(4)} z_1^2 = \Delta_{\text{mod}} |d_{\mathbf{k}}|, \quad (46)$$

with

$$\Delta_{\text{mod}} = -\frac{V}{2N z_1^2} \sum_{\mathbf{k},\sigma} |d_{\mathbf{k}}| \sigma \langle c_{\mathbf{k},\sigma}^\dagger c_{\mathbf{k}+\mathbf{Q},\sigma} \rangle. \quad (47)$$

We introduce the unitary matrix  $U(\mathbf{k})$  that diagonalizes the Hamiltonian Eq. (42):

$$U(\mathbf{k}) \begin{pmatrix} \eta_1(\mathbf{k}) & \eta_2(\mathbf{k}) \\ \eta_2(\mathbf{k}) & \eta_3(\mathbf{k}) \end{pmatrix} U(\mathbf{k})^\dagger = \begin{pmatrix} E_-(\mathbf{k}) & 0 \\ 0 & E_+(\mathbf{k}) \end{pmatrix}. \quad (48)$$

The self-consistent gap equation is given by Eqs. (46,47) and takes the form (at half filling)

$$\begin{aligned} \Delta_{\mathbf{k}}^{(4)} &= -\frac{V}{2N} |d_{\mathbf{k}}| \sum_{\mathbf{k}',\sigma} |d_{\mathbf{k}'}| \sigma \langle c_{\mathbf{k}',\sigma}^\dagger c_{\mathbf{k}+\mathbf{Q},\sigma} \rangle \\ &= -\frac{V}{2N} |d_{\mathbf{k}}| \sum_{\mathbf{k}',\sigma}^{\text{AF}} |d_{\mathbf{k}'}| \sigma \\ &\times \left[ U(\mathbf{k}) \begin{pmatrix} 2z_1 z_2 \sigma & z_1^2 + z_2^2 \\ z_1^2 + z_2^2 & 2z_1 z_2 \sigma \end{pmatrix} U(\mathbf{k})^\dagger \right]_{1,1}. \end{aligned} \quad (49)$$

The ground-state energy

$$E = H_{bos} + \sum_{\mathbf{k},\sigma}^{\text{AF}} E_1(\mathbf{k}) \quad (50)$$

then has to be minimized with respect to the saddle-point values of the fields  $d, e, p_1, p_2, \lambda_1, \lambda_2$  and  $\lambda_3$ . Along with the gap-equation Eq. (49) this gives 8 coupled equations that are readily solved numerically.

## B. SC phase

The Slave-boson calculation in the superconducting phase is very similar to (in fact simpler than) the one in the AF phase. Therefore, we will skip details and only show the main differences. Indeed, in this case we can use the paramagnetic *ansatz* for the bosons which avoids the complication of two different sublattices:

$$\begin{aligned}
d_r(\tau) &= d \\
e_r(\tau) &= e \\
p_{r,\sigma}(\tau) &= p \\
\lambda_r^{(1)} &= i\lambda_1 \\
\lambda_r^{(2)} &= i\lambda_2.
\end{aligned} \tag{51}$$

$z_r$  is obviously independent of  $\sigma$  and is given again by Eq. (34). The saddle-point approximation yields the mean-field Hamiltonian (the counterpart of equation (38)):

$$\begin{aligned}
H_{\text{SBMF}} &= N\lambda_1 e^2 - N\lambda_1 + 2Np^2(\lambda_1 - \lambda_2) \\
&+ Nd^2(\lambda_1 - 2\lambda_2 + U) \\
&+ \sum_{\mathbf{k},\sigma} f_{\mathbf{k},\sigma}^\dagger (\varepsilon(\mathbf{k})z^2 + \lambda_2 - \mu) f_{\mathbf{k},\sigma} + H_{\text{SO}(5),I}. \tag{52}
\end{aligned}$$

In the SC phase, the SO(5) part reads

$$H_{\text{SO}(5),I} = z^2 \sum_{\mathbf{k}} \Delta_{\mathbf{k}}^{(1)} \left( f_{\mathbf{k},\uparrow}^\dagger f_{-\mathbf{k},\downarrow}^\dagger - f_{\mathbf{k},\uparrow} f_{-\mathbf{k},\downarrow} \right), \tag{53}$$

with the condition

$$\Delta_{\mathbf{k}}^{(1)} = -\frac{V}{2N} d_{\mathbf{k}} \sum_{\mathbf{k}'} d_{\mathbf{k}'} \langle c_{\mathbf{k}',\uparrow}^\dagger c_{-\mathbf{k}',\downarrow}^\dagger - c_{\mathbf{k}',\uparrow} c_{-\mathbf{k}',\downarrow} \rangle. \tag{54}$$

The purely fermionic part

$$\begin{aligned}
H_F &= \sum_{\mathbf{k},\sigma} f_{\mathbf{k},\sigma}^\dagger [\varepsilon(\mathbf{k})z^2 + \lambda_2 - \mu] f_{\mathbf{k},\sigma} \\
&+ z^2 \sum_{\mathbf{k}} \Delta_{\mathbf{k}}^{(1)} \left( f_{\mathbf{k},\uparrow}^\dagger f_{-\mathbf{k},\downarrow}^\dagger - f_{\mathbf{k},\uparrow} f_{-\mathbf{k},\downarrow} \right) \tag{55}
\end{aligned}$$

can be diagonalized by the usual Bogoliubov transformation. This yields the eigenvalues

$$\pm E(\mathbf{k}) = \pm \sqrt{(\varepsilon(\mathbf{k})z^2 + \lambda_2 - \mu)^2 + (\Delta_{\mathbf{k}}^{(1)})^2}. \tag{56}$$

Calculating the expectation value of the order parameter in the ground state, constructed from the Bogoliubov eigenstates, gives a self-consistent gap equation in the usual form:

$$1 = \frac{V}{2N} z^4 \sum_{\mathbf{k}} d_{\mathbf{k}}^2 \frac{1}{\sqrt{(\varepsilon(\mathbf{k})z^2 + \lambda_2 - \mu)^2 + \Delta_{\text{SC}}^2 d_{\mathbf{k}}^2 z^4}}, \tag{57}$$

where  $\Delta_{\text{SC}}$  is the amplitude of the modulation

$$\Delta_{\mathbf{k}}^{(1)} = d_{\mathbf{k}} \Delta_{\text{SC}}. \tag{58}$$

The gaps obtained from the slave-boson calculation are reported in Figs. 2, and 7.

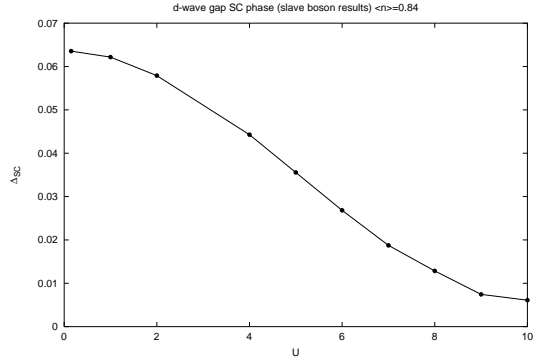


FIG. 7. The  $d$ -wave gap  $\Delta_{\text{SC}}$  in the superconducting phase with density  $\langle n \rangle = 0.84$  as a function of the Hubbard interaction  $U$  for fixed  $V = 0.61 t$ . We see that, in contrast to the antiferromagnetic phase,  $U$  lowers the value of the gap.

Figure 2 shows the behavior of the AF gap modulation as a function of  $U$ . Just like in the simple Hartree-Fock type of mean field described in Sec. A 2, we observe that increasing the Hubbard-interaction  $U$  enhances the  $d$ -wave-like modulation  $\Delta_{\text{mod}}$  of the AF gap at half filling, and, eventually, saturates around  $U/t \approx 8 - 10$ . The *dispersion* of the gap is of course identical to the Hartree-Fock mean-field result, Fig. 4.

The superconducting phase has again a  $d$ -wave structure. However, in contrast to the simple Hartree-Fock mean field, where  $U$  was of no influence, the Hubbard interaction  $U$  results in a *suppression* of the superconducting gap  $\Delta_{\text{SC}}$  at finite doping, as shown in Fig. 7. This is due to the well-known reduction of the effective hopping produced by the slave-boson formulation. The combination of these two effects with increasing  $U$  (enhancement of  $\Delta_{\text{mod}}$  in the AF phase and suppression of  $\Delta_{\text{SC}}$  in the SC phase) yields a ratio of the two gaps  $\Delta_{\text{mod}}/\Delta_{\text{SC}}$  of the order of 10, slightly larger than the Hartree-Fock calculation, and more in agreement with experimental findings.

## V. SUMMARY

Summarizing, we have shown that the  $|d|$ -wave-like modulation observed in the AF gap at half filling in  $\text{Ca}_2\text{CuO}_2\text{Cl}_2$ , similar to the dispersion of the SC gap at finite doping, indicates an intimate relationship between the two phases, as suggested by the SO(5) theory of high- $T_c$  superconductivity. The idea is that one gap can be mapped into the other by a SO(5) transformation. This is done by using an effective SO(5)-invariant Hamiltonian which allows for such a mapping. However, we have also shown that it is important to break this symmetry by introducing “by hand” an Hubbard interaction term in order to correctly obtain the constant part of the AF gap. Via this “projected” SO(5) theory, we can interpret the experimentally observed  $d$ -wave-like modulation of the AF gap as the fingerprint of the superconductor in

the AF state just like the neutron resonance mode<sup>30–32</sup> may be viewed as the fingerprint of the AF correlation in the SC state<sup>33</sup>.

The projection can also explain the experimentally observed order of magnitude difference between the  $d$ -wave-like gap modulation in the AF state ( $\approx J \sim 0.12\text{eV}$ ) and the  $d$ -wave gap in the SC state ( $\approx J/10$ ). This different magnitude of the two gap modulations also suggests a reason why the Néel temperature differs so much from the superconducting transition temperature.

Finally, we have shown that the projected SO(5) theory can provide a qualitative explanation for the observation<sup>15</sup>, that the maximum  $T_c$  observed in a large variety of high- $T_c$  cuprates scales with the next-nearest-neighbor hopping matrix element  $t'$ .

## ACKNOWLEDGMENTS

We thank Z. C. Zhang, R.B. Laughlin, D.J. Scalapino, R. Eder, Z.-X. Shen, J. C. Campuzano and O.K. Andersen for helpful discussions and suggestions. We acknowledge financial support by the DFG [HA 1537/17-1, HA1537/16-2, and partially from the Heisenberg program AR 324/3-1 (EA)], KONWIHR OOPCV, and BMBF (05SB8WWA1). This work is dedicated to Professor E. Müller-Hartmann on the occasion of his 60<sup>th</sup> birthday.

- 
- <sup>1</sup> S.-C. Zhang, *Science* **275**, 1089 (1997).
  - <sup>2</sup> E. Arrigoni and W. Hanke, *Phys. Rev. Lett.* **82**, 2115 (1999).
  - <sup>3</sup> R. Eder, W. Hanke, and S.-C. Zhang, *Phys. Rev. B* **57**, 13781 (1998).
  - <sup>4</sup> S. Meixner, W. Hanke, E. Demler, and S.-C. Zhang, *Phys. Rev. Lett.* **79**, 4902 (1997).
  - <sup>5</sup> W. Hanke, R. Eder, E. Arrigoni, A. Dorneich, S. Meixner, and M. G. Zacher, in *Festkörper Probleme/Advances in Solid State Physics*, edited by B. Kramer (Vieweg, Braunschweig, 1999), Vol. 38.
  - <sup>6</sup> W. Hanke, R. Eder, E. Arrigoni, A. Dorneich, and M. G. Zacher, *Physica C* **317**, 175 (1999).
  - <sup>7</sup> H.-H. Lin, L. Balents, and M. P. A. Fisher, *Phys. Rev. B* **58**, 1794 (1998).
  - <sup>8</sup> S.-C. Zhang, J.-P. Hu, E. Arrigoni, W. Hanke, and A. Auerbach, *Phys. Rev. B* **60**, 13070 (1999).
  - <sup>9</sup> M. G. Zacher, W. Hanke, E. Arrigoni, and S.-C. Zhang, *Phys. Rev. Lett.* **85**, 824 (2000).
  - <sup>10</sup> A. Dorneich, W. Hanke, E. Arrigoni, M. Troyer, and S. C. Zhang, to appear in *Phys. Rev. Lett.* (cond-mat/0106473).
  - <sup>11</sup> A. Ino, T. Mizokawa, A. Fujimori, K. Tamasaku, H. Eisaki, S. Uchida, T. Kimura, T. Sasagawa, and K. Kishio, *Phys. Rev. Lett.* **79**, 2101 (1998).

- <sup>12</sup> B. O. Wells, Y. S. Lee, M. A. Kastner, R. J. Christianson, R. J. Birgeneau, K. Yamada, Y. Endoh, and G. Shirane, *Science* **277**, 1067 (1997).
- <sup>13</sup> E. Arrigoni and W. Hanke, *Phys. Rev. B* **62**, 11770 (2000).
- <sup>14</sup> S. Rabello, H. Kohno, E. Demler, and S.-C. Zhang, *Phys. Rev. Lett.* **80**, 3586 (1998).
- <sup>15</sup> E. Pavarini, I. Dasgupta, T. Saha-Dasgupta, O. Jepsen, and O. K. Andersen, *Phys. Rev. Lett.* **87**, 047003 (2001).
- <sup>16</sup> F. Ronning, C. Kim, D. L. Feng, D. S. Marshall, A. G. Loeser, L. L. Miller, J. N. Eckstein, I. Bozovic, and Z.-X. Shen, *Science* **282**, 2067 (1998).
- <sup>17</sup> D. S. Marshall, D. S. Dessau, A. G. Loeser, C.-H. Park, A. Y. Matsuura, J. N. Eckstein, I. Bozovic, P. Fournier, A. Kapitulnik, W. E. Spicer, and Z.-X. Shen, *Phys. Rev. Lett.* **76**, 4841 (1996).
- <sup>18</sup> P. J. White, Z.-X. Shen, C. Kim, J. M. Harris, A. G. Loeser, P. Fournier, and A. Kapitulnik, *Phys. Rev. B* **54**, R15669 (1996).
- <sup>19</sup> H. Ding, T. Yokoya, J. C. Campuzano, T. Takahashi, M. Randeria, M. R. Norman, T. Mochiku, K. Kadowaki, and J. Giapintzakis, *Nature (London)* **382**, 51 (1996).
- <sup>20</sup> J. Mesot, M. R. Norman, H. Ding, M. Randeria, J. C. Campuzano, A. Paramekanti, H. M. Fretwell, A. Kaminski, T. Takeuchi, T. Yokoya, T. Sato, T. Takahashi, T. Mochiku, and K. Kadowaki, *Phys. Rev. Lett.* **83**, 840 (1999).
- <sup>21</sup> R. Eder, *Phys. Rev. B* **59**, 13810 (1999).
- <sup>22</sup> C. L. Henley, *Phys. Rev. Lett.* **80**, 3590 (1998).
- <sup>23</sup> C. Kim, P. J. White, Z.-X. Shen, T. Tohyama, Y. Shibata, S. Maekawa, B. O. Wells, Y. J. Kim, R. J. Birgeneau, and M. A. Kastner, *Phys. Rev. Lett.* **80**, 4245 (1998).
- <sup>24</sup> R. B. Laughlin, *Phys. Rev. Lett.* **79**, 1726 (1997).
- <sup>25</sup> G. Kotliar and A. E. Ruckenstein, *Phys. Rev. Lett.* **57**, 1362 (1986).
- <sup>26</sup> E. Arrigoni and G. C. Strinati, *Phys. Rev. Lett.* **71**, 3178 (1993).
- <sup>27</sup> E. Arrigoni and G. C. Strinati, *Phys. Rev. B* **52**, 2428 (1995).
- <sup>28</sup> E. Arrigoni and G. C. Strinati, *Phys. Rev. B* **52**, 13707 (1995).
- <sup>29</sup> L. Lilly, A. Muramatsu, and W. Hanke, *Phys. Rev. Lett.* **65**, 1379 (1990).
- <sup>30</sup> J. Rossat-Mignod, L. P. Regnault, C. Vettier, P. Bourges, P. Burlet, J. Bossy, J. Y. Henry, and G. Lepertot, *Physica C* **185–198**, 86 (1991).
- <sup>31</sup> H. A. Mook, M. Yethiraj, G. Aeppli, T. E. Mason, and T. Armstrong, *Phys. Rev. Lett.* **70**, 3490 (1993).
- <sup>32</sup> H. F. Fong, B. Keimer, P. W. Anderson, D. Reznik, F. Dogan, and I. A. Aksay, *Phys. Rev. Lett.* **75**, 316 (1995).
- <sup>33</sup> E. Demler and S.-C. Zhang, *Nature (London)* **396**, 733 (1998).

## APPENDIX A: DETAILS OF THE MEAN-FIELD CALCULATIONS

### 1. BCS solution of the SC state

At finite doping, the symmetry between SC and AF is broken to favor SC. Therefore, we look for a BCS solu-

tion given by a finite mean-field expectation value of the operator  $\Delta$  in Eq. (12). The Hamiltonian, Eq. (17), becomes quadratic in the fermionic operators and can be solved by the usual Bogoliubov transformation. The mean-field condition results in the BCS gap equation for the amplitude of the order parameter  $\Delta_{SC}$ , i. e.

$$1 = \frac{V}{N} \sum_{\mathbf{k}} \frac{d_{\mathbf{k}}^2}{2\sqrt{(\varepsilon_{\mathbf{k}} - \mu)^2 + \Delta_{SC}^2 d_{\mathbf{k}}^2}}, \quad (\text{A1})$$

which has to be solved in a self-consistent way for a given value of the parameter  $V$ . Notice that the on-site interaction  $U$  does not enter this equation, due to the fact that, in contrast to  $s$ -wave, two holes of a  $d$ -wave pair never occupy the same site.

The  $k$ -dependent SC gap is given by  $\Delta_{SC} d_{\mathbf{k}}$  and depends on two parameters: the magnitude  $\Delta_{SC}$  and the parameter  $b$  introduced in Eq. (9), giving its shape. Our procedure consists in fitting these two parameters to the recent data on the SC gap by Mesot et al.<sup>20</sup>. In that paper, the SC gap obtained by ARPES experiments was fitted with a  $d$ -wave form including nearest- and next-nearest-neighbor terms:

$$d_{\mathbf{k}} = b(\cos k_x - \cos k_y) + (1 - b)(\cos 2k_x - \cos 2k_y). \quad (\text{A2})$$

This form cannot be made consistent with our SO(5) hypothesis, since it would require a form factor Eq. (8) without the property  $g_{\mathbf{k}+\mathbf{Q}} = -g_{-\mathbf{k}}$ . However, a fit of the SC gap by the form, Eq. (9), turns out to be as good as one from the next-nearest-neighbor form, Eq. (A2).

Our best fit to the data of Ref. 20 with Eq. (9) gives  $b = 0.81$ , and  $\Delta_{SC} = 0.04t$ . The values of the parameters can be inserted in Eq. (A1) to obtain the appropriate value of  $V$  ( $V = 0.89t$ ), which can now be used to study the AF phase.

## 2. Hartree-Fock solution for the Antiferromagnetic phase

We now look for the AF solution of the mean-field equation for the Hamiltonian, Eq. (17), at half filling. This is slightly more complicated than the BCS result, Eq. (A1), due to the interplay between the SO(5) interaction in Eq. (13) and the Hubbard repulsion term.

We introduce a momentum dependent SDW operator polarized in the  $z$ -direction:

$$n_{\mathbf{k}} = c_{\mathbf{k}+\mathbf{Q}}^\dagger \sigma^z c_{\mathbf{k}} = 2N_3(\mathbf{k}). \quad (\text{A3})$$

Within a mean-field decoupling, the Hamiltonian in Eq. (17) becomes

$$\begin{aligned} H_{\text{MF}} &= \sum_{\mathbf{k},\sigma} \varepsilon(\mathbf{k}) c_{\mathbf{k},\sigma}^\dagger c_{\mathbf{k},\sigma} - \frac{U}{2N} \left[ \sum_{\mathbf{k}'} \langle n_{\mathbf{k}'} \rangle \right] \sum_{\mathbf{k}} n_{\mathbf{k}} \\ &\quad - \frac{V}{2N} \left[ \sum_{\mathbf{k}'} |d_{\mathbf{k}'}| \langle n_{\mathbf{k}'} \rangle \right] \sum_{\mathbf{k}} |d_{\mathbf{k}}| n_{\mathbf{k}} \\ &= \sum_{\mathbf{k},\sigma} \varepsilon(\mathbf{k}) c_{\mathbf{k},\sigma}^\dagger c_{\mathbf{k},\sigma} - \Delta_U \sum_{\mathbf{k}} n_{\mathbf{k}} \\ &\quad - \Delta_{\text{mod}} \sum_{\mathbf{k}} |d_{\mathbf{k}}| n_{\mathbf{k}}, \end{aligned} \quad (\text{A4})$$

with the self-consistent parameters

$$\Delta_U = \frac{U}{2N} \left[ \sum_{\mathbf{k}'} \langle n_{\mathbf{k}'} \rangle \right], \quad (\text{A5})$$

$$\Delta_{\text{mod}} = \frac{V}{2N} \left[ \sum_{\mathbf{k}'} |d_{\mathbf{k}'}| \langle n_{\mathbf{k}'} \rangle \right]. \quad (\text{A6})$$

It is convenient to recast equation (A4) in matrix form as a sum over the antiferromagnetic Brillouin zone (AFBZ),

$$H = \sum_{\mathbf{k},\sigma}^{AFBZ} \begin{pmatrix} c_{\mathbf{k},\sigma} \\ c_{\mathbf{k}+\mathbf{Q},\sigma} \end{pmatrix}^\dagger \cdot M(\mathbf{k}) \cdot \begin{pmatrix} c_{\mathbf{k},\sigma} \\ c_{\mathbf{k}+\mathbf{Q},\sigma} \end{pmatrix}, \quad (\text{A7})$$

with

$$M(\mathbf{k}) = \begin{pmatrix} \varepsilon(\mathbf{k}) & -\sigma(\Delta_U + \Delta_{\text{mod}} |d_{\mathbf{k}}|) \\ -\sigma(\Delta_U + \Delta_{\text{mod}} |d_{\mathbf{k}}|) & -\varepsilon(\mathbf{k}) \end{pmatrix}. \quad (\text{A8})$$

The Hamiltonian (equation (A7)) can be diagonalized by the usual transformation into Bogoliubov operators

$$\begin{aligned} \gamma_{\mathbf{k},\sigma}^c &= u_{\mathbf{k}} c_{\mathbf{k},\sigma} + \sigma v_{\mathbf{k}} c_{\mathbf{k}+\mathbf{Q},\sigma}, \\ \gamma_{\mathbf{k},\sigma}^v &= v_{\mathbf{k}} c_{\mathbf{k},\sigma} - \sigma u_{\mathbf{k}} c_{\mathbf{k}+\mathbf{Q},\sigma} \end{aligned} \quad (\text{A9})$$

with amplitudes

$$\begin{aligned} u_{\mathbf{k}} &= \frac{1}{\sqrt{2}} \sqrt{1 + \frac{\varepsilon(\mathbf{k})}{E(\mathbf{k})}}, \\ v_{\mathbf{k}} &= \frac{1}{\sqrt{2}} \sqrt{1 - \frac{\varepsilon(\mathbf{k})}{E(\mathbf{k})}}, \end{aligned} \quad (\text{A10})$$

and eigenvalues

$$\pm E(\mathbf{k}) = \pm \sqrt{\varepsilon(\mathbf{k})^2 + (\Delta_U + |d_{\mathbf{k}}| \Delta_{\text{mod}})^2}. \quad (\text{A11})$$

At half-filling, the ground state consists of all states of  $\gamma^c$  particles occupied ( $c$  stands for *conduction* band with  $E(\mathbf{k}) < 0$  and  $v$  for *valence* band with  $E(\mathbf{k}) > 0$ ) and the expectation value  $\langle n_{\mathbf{k}} \rangle$  can be readily evaluated.